DETAILED INVESTIGATION IN DEVELOPMENTAL PROCESS OF FULL ANNULAR COMBUSTOR FOR SMALL AIRCRAFT JET ENGINE

Mitsumasa MAKIDA, Hideshi YAMADA and Kazuo SHIMODAIRA*
*** Japan Aerospace Exploration Agency**

Keywords: *Full annular combustor, NOx reduction,Exit Temperature Profile, Rich-Lean*

Abstract

In the TechCLEAN project of JAXA, experimental research has been conducted to develop a combustor for a small aircraft engine. The combustor was tuned to show the behavior of the Rich-Lean combustion through tests under atmospheric and practical conditions. And finally, through full annular combustion experiments under practical conditions, the combustor was tuned to reduce NOx emissions to lower than 40% of the ICAO CAEP4 standard, also sustaining low CO and UHC emissions. To investigate the performance of the full annular combustor in detail, parametric experiments were conducted under additional test conditions. Also, some of fuel nozzles were replaced with modified type and compared with original one. Obtained results such as emission characteristics and exit temperature distributions are discussed in this report.

1 INTRODUCTION

In general, small and medium power aircraft engines must simultaneously satisfy several requirements, for example, high efficiency, environmental friendliness and cost effectiveness [1]. In October 2003, Japan Aerospace Exploration Agency (JAXA) started a project "Technology development project for clean engines" (so-called TechCLEAN project), in which researches to develop advanced combustion technology were conducted aiming to reduce toxic exhaust gas components, especially NOx, from aeroengine combustors. And in the framework of the TechCLEAN project, JAXA has been developing aeroengine combustors for an affordable and environment-friendly small aircraft (with approximately 50-passengers). The designed thrust of the engine is about 40kN and the pressure ratio is about 20, and the target of the combustor development is to reduce NOx emissions lower than 50% of the ICAO CAEP4 standard, aiming to precede the trend of NOx emissions shown in the lower right of Fig.1, with NOx emissions level achieved in this research. And also to reduce CO and UHC emissions to those of 90% and ensure basic performance of aero engine combustors, such as ignition and blow-out.

An overview of the development process of our combustor, shown in Fig.1, was already introduced in the previous report [2-4]. The upper left figure of Fig.1 shows a cross-sectional drawing of the combustor with description explaining the preliminary design concept. For this combustor, both the reduction of NOx emissions with high combustion efficiency over a wide range of operating conditions [5], and the reduction of direct operating cost (DOC) are required. To satisfy this requirement, the Rich-Lean combustion approach [6] was utilized for this combustor, and we applied the concept of single fuel supplied airblast type nozzles proposed by Parker-Hannifin [7], as shown in Fig.1a. In the combustor design mentioned above, two factors should play significant rolls; the enhanced mixing in the primary combustion region, and the tuning of the air mass flow ratio among the fuel nozzle, the primary and secondary combustion regions and the wall cooling. A lot of research has been done on these factors [8-14], and also in our research, a large portion of effort has been concentrated on them.

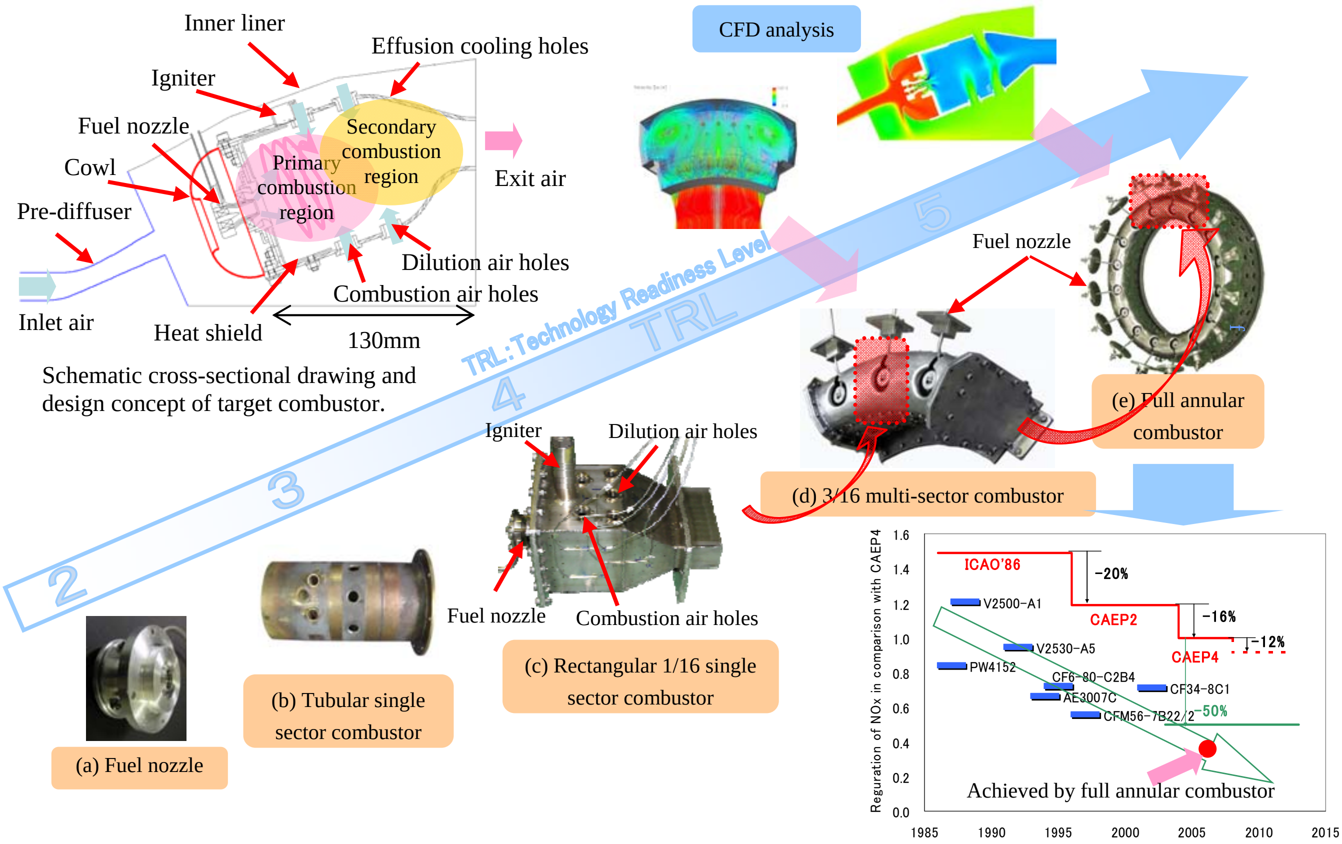

Trend of NOx emissions and achieved level of NOx reduction with ICAO standards.

Fig.1. Overview of development process of aircraft combustor.

2 Review of Combustor Development Process

In the preliminary emission tests with tubular combustors (Fig.1b) under atmospheric pressure, the air mass flow ratio was tuned to show the Rich-Lean behavior, that is, reducing NOx emissions at low AFR (Air to Fuel Ratio) condition, also sustaining high combustion efficiency. The emission tests were conducted for more than 20 cases with different air hole locations and sizes.

Based on the designed air mass flow ratio, rectangular single-sector combustors were designed (Fig.1c). To compare emission results with the ICAO CAEP4 standard, combustion tests were conducted under the inlet temperature, pressure and mass flow rate which were set to simulate the operating conditions corresponding to the ICAO LTO (Landing and Take-Off) cycle; 7%, 30%, 85% and 100% thrust of MTO (Max Take-Off) design points of the target engine. The level of NOx emissions was reduced to 44.3% of the ICAO CAEP4 standard and achieved the emission target, while UHC emission exceeded the target slightly.

Following the results of the tubular and rectangular single-sector combustor tests, multi-sector combustors with three fuel nozzles (Fig.1d) were designed, simulating 3/16 region of the target combustor. Staggered allocation type was applied for combustion air holes. Combustion tests were also conducted under practical conditions mentioned before, and NOx emissions were reduced by almost 40% of ICAO CAEP4, and UHC and CO emissions were reduced much lower than the standard.

Then based on the design of the multi-sector combustor, full annular combustors were designed. Figure 1e shows a photograph of the full annular combustor linear FA1-1, equipped with 16 fuel nozzles. Through combustion tests under practical conditions, the combustion characteristics were tried to be adjusted to those of the multi-sector combustor, by tuning the size of the combustion and dilution air holes. This modification was applied to the second full annular combustor FA1-2 and successfully

Table 1. Comparison of emission summation in ICAO LTO cycle among full annular combustors FA1-2, FA2-N1, FA2-N2 and target level in percentage figures of ICAO CAEP4 standard.

	NOx	UHC	CO
Target	50.0%	90.0%	90.0%
FA1-2	38.1%	16.3%	60.1%
FA2-N1	43.1%	1.9%	57.2%
FA2-N2	42.3%	3.0%	58.6%

Table 2. High temperature and high pressure inlet air conditions of parametric tests of full annular combustor.

Temperature (K)	Pressure (kPa)	Mass flow rate (kg/s)	AFR
450	315.3	4.16	95.3
500	503.7	6.44	84.3
550	738.1	8.86	73.2
600	1,018.4	11.44	62.1
650	1,344.7	14.18	51.0

adjusted the mass flow ratio to that of the multi-sector combustor, and the emission plots also became closer. And for the summation over the ICAO LTO cycle, which is shown in Table 1, NOx emissions were successfully reduced to 38.1% of the ICAO CAEP4 standard.

3 Detailed Measurements of Full Annular Combustor under Practical Conditions

3.1 Modification of Full Annular Combustor and Test Conditions

In previous experiments described before, combustion tests were only conducted under ICAO LTO cycle conditions of the target engine. In order to obtain more detailed data, we also conducted parametric combustion tests of a full annular combustor FA2 with inlet temperature increasing from 450K to 650K with intervals of 50K. Also inlet pressure and air mass flow rate conditions were changed along the design line of the target engine, as shown in Table.2.

The combustor FA2 itself was also modified from FA1-2, by slightly decreasing the dilution air holes (about 2.5% of total opening area) and increasing the wall cooling air holes in the same area, that is, both the total opening area of the combustor linear and the air flow ratio from the fuel nozzle were not changed.

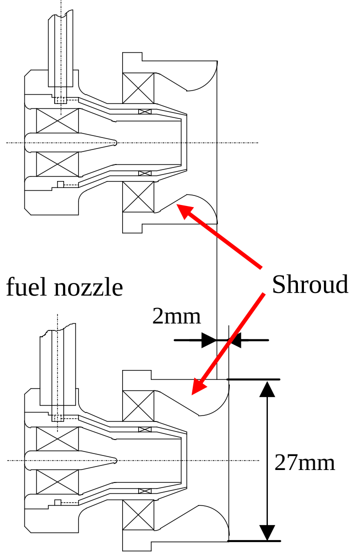

Fig.2. Difference between fuel nozzles N1 and N2.

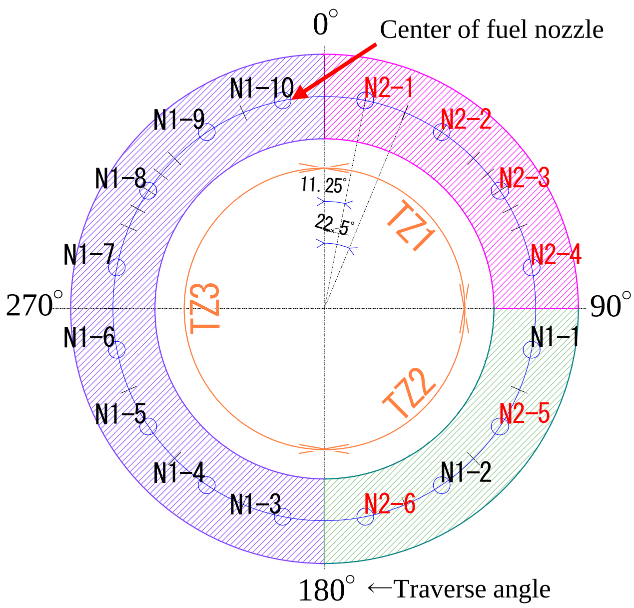

Fig.3. Schematic drawing of fuel nozzle allocation and segmentation of traverse zone into TZ1, TZ2 and TZ3. (Viewing from downstream of combustor exit.)

And we also applied modified fuel nozzles. Two types of fuel nozzles are shown in Fig.2; (a) the original type N1 and (b) modified type N2. The shroud of N2 was extended by 2mm aiming to improve fuel atomization. To see the difference between N1 and N2 nozzles, and also to see mixed effect of them, ten N1 nozzles and six N2 nozzles were allocated circumferentially as shown in Fig.3. In the traverse measurements

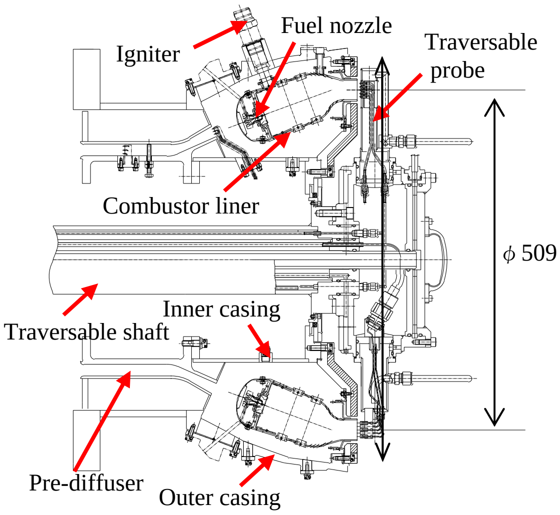

Fig.4. Schematic drawing of full annular combustor with traversable measurement system.

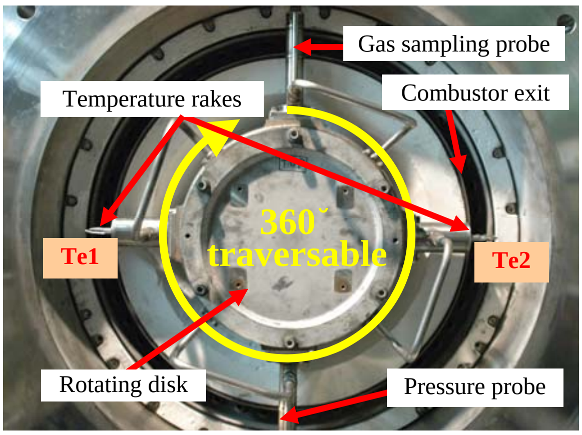

Fig.5. Temperature rakes Te1 and Te2, gas and pressure sampling probes traversable at combustor exit.

at the combustor exit, rake angle from 0 to 90 degrees corresponds to the traverse zone TZ1 with N2 nozzles, from 90 to 180 degrees corresponds to TZ2 with N1 and N2 nozzles mixed, and from 180 to 360 degrees corresponds to TZ3 with N1 nozzles.

3.2 Full Annular Combustor Test Facility and Traversable Measurement System

Combustion tests of the full annular combustor FA2 were conducted under the practical operating conditions at the "High-Temperature and Pressure Full Annular Combustor Test Facility" which was developed by JAXA in the spring of 2007. The detail of this facility was already introduced in the previous report [4], but some specifications relating to the detailed measurements in this report are mentioned here again. In Fig.4, a schematic drawing of the cross-section of the test facility near the full annular combustor is shown. This test facility has a traversable measuring system at the combustor exit. As shown in Fig.5, exhaust gas concentration, pressure and temperature distributions at the combustor exit are measured by the gas sampling and pressure probes and two temperature sensor rakes. They are mounted on the 360 degrees rotating disk located at the combustor exit. Each probe and rake has five sampling points in the radial direction. As shown in Fig.4, the rotating disk is connected to the drive motor by the long traverse shaft passing through the combustion test section. It can be rotated within a range of ±185 degrees and has feedback control with the accuracy of 0.5 degrees. The rotating disk, the gas sampling probes and the temperature sensor rakes are cooled by pressurized water provided through the traverse shaft. Sampled gas from the collective 5 points probes is led through the shaft, being kept warm by pressurized hot water (3MPa, 430K), and led to the gas analyzers through a heated sampling line. These gas sampling procedures are based on the ICAO standards [15].

3.3 Results of Detailed Measurement: Emission Characteristics

As mentioned above, combustion tests of FA2 were conducted under parametric conditions shown in Table.2, but to compare its combustion characteristics with those of FA1-2, combustion tests were also conducted under ICAO LTO cycle conditions (which cannot be shown here). Obtained NOx emissions and combustion efficiency of FA1-2, FA2-N1 and FA2-N2 are shown in Fig.6. Here, “EINOx” means grams of NOx emitted per 1kg fuel, and each vertical dotted line noted as ①-④ shows the designed AFR at each condition of the LTO cycle respectively. The exhaust gas was measured downstream of one nozzle only, varying fuel mass flow (that is, AFR). FA1-2 was equipped with N1 nozzles, and FA2-N1 was measured at 303.75 degrees traverse angle, and FA2-N2 was measured at 56.25 degrees.

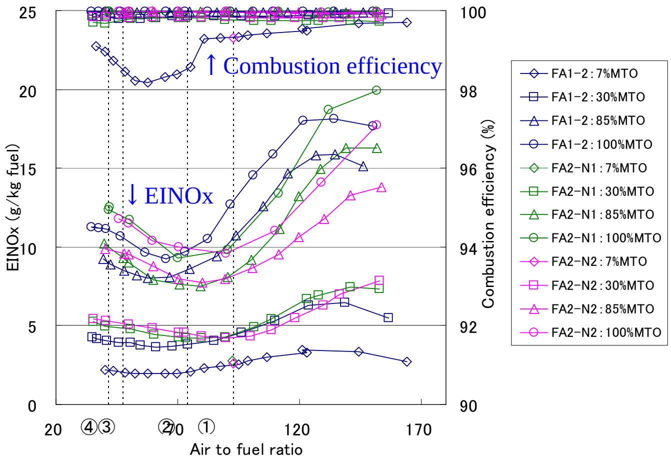

Fig.6. Emission characteristics of FA1-2 and FA2-N1 under LTO cycle conditions.

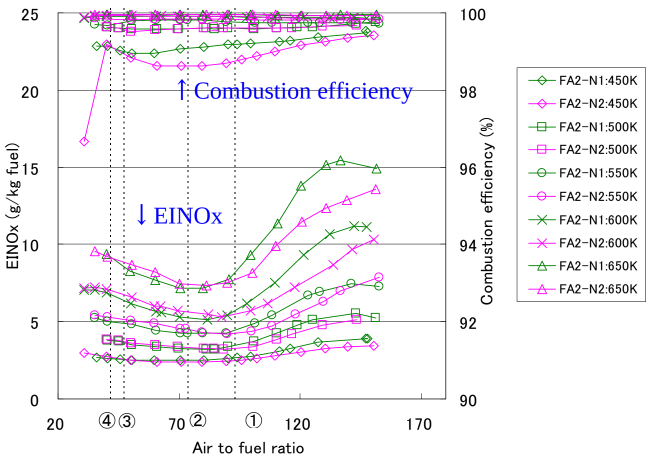

Fig.7. Emission characteristics of FA2-N1 and FA2-N2 under parametric test conditions.

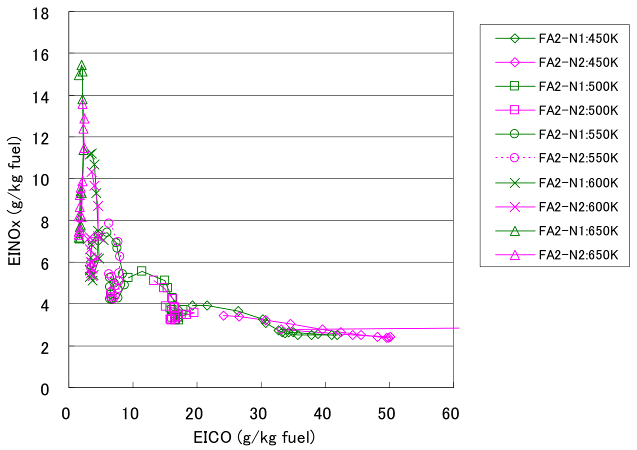

Fig.8. Correlation of CO-NOx emissions of FA2-N1 and FA2-N2 under parametric test conditions.

And here, emission measurements of FA2 under 7%MTO conditions were conducted at the designed AFR only. From this graph, we can see that the combustion efficiency of FA2-N1 was improved from that of FA1-2, but the center of the NOx plots were shifted to higher AFR range and the slope of the plots got steeper. Comparing the plots of NOx between FA2-N1 and FA2-N2, the slope of FA2-N2 was gentler in high AFR range, but almost the same or little higher in low AFR range. So at the designed AFR of 30%, 85% and 100%MTO conditions, NOx emissions of FA2-N1 and FA2-N2 were higher than those of FA1-2. Therefore, for the summation over the ICAO LTO cycle, which is shown in Table 1, NOx emissions increased and UHC emission were largely decreased for both FA2-N1 and FA2-N2 than those of FA1-2.

For the comparison between FA2-N1 and FA2-N2 under the parametric conditions of Table.2, plots of NOx emissions and combustion efficiency versus AFR are shown in Fig.7, and the correlation of CO-NOx emissions are also plotted in Fig.8. As mentioned before, the slopes of NOx plots of FA2-N2 were gentler in high AFR range, but got slightly higher in low AFR range. This means, the improvement of fuel atomization by N2 nozzle suppressed NOx emissions at high AFR (fuel lean) conditions, but had some inverse effect at low AFR (fuel rich) conditions. And for FA2-N2, CO emission was slightly higher and the combustion efficiency was lower than FA2-N1, especially under low inlet temperature conditions.

3.4 Results of Detailed Measurement: Exit Temperature Distribution

In addition to the emission characteristics shown above, the temperature distribution at the combustor exit is also one of the very important performances, required from the design of turbine blades. Therefore, detailed measurements were conducted for the exit temperature distributions under the parametric conditions shown in Table.2. As mentioned before, to obtain temperature distribution at the exit of the combustor, the test facility has two traversable temperature rakes mounted axially symmetry with 180 degrees as shown in Fig.5, and each rake has five sampling points, equally-spaced in the radial direction. The traverse measurements were conducted based on the

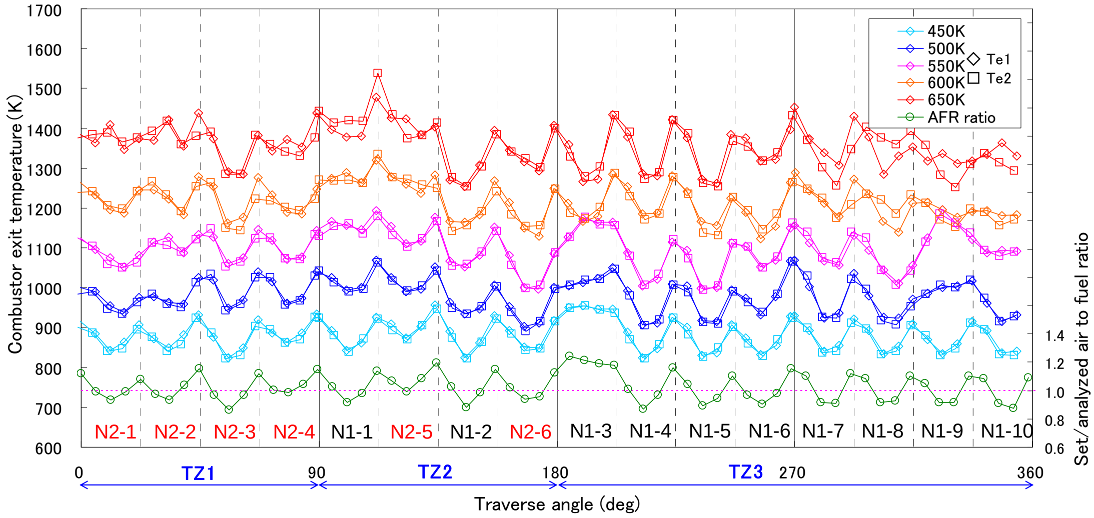

Fig.9. Circumferential profiles of temperature and AFR ratio at combustor exit of FA2 under parametric test conditions, shown with traverse zones and fuel nozzle allocation.

position of the gas sampling probe, and started from 0 degree for the probe, traversed in the clockwise direction (as shown by the yellow arrow in Fig.5) at the interval of 5.6 degrees. So each rake of Te1 and Te2 started from 270 and 90 degrees. This means that the data of Te1 and Te2 obtained at same angular position were measured with the interval of traverse for 180 degrees, which took about 15 minutes during these experiments. So the difference of Te1 and Te2 in the circumferential distribution indicates the fluctuation of the combustion condition during the traverse measurements, including the deviation of inlet air conditions.

Figure 9 shows the circumferential exit temperature distribution measured by the temperature sensor rakes and averaged over the five points in the radial direction for both Te1 and Te2, under each condition shown in Table.2. And the ratio of the set AFR and the analyzed AFR calculated from the measured gas concentration under the 450K condition is also plotted. This ratio indicates the uniformity of the fuel distribution. And two-dimensional (radial and circumferential) distributions of combustor exit temperature, measured by five sampling points on the rake Te1 are shown in Fig.10. In these figures, polar plots of averaged Te1 and Te2 are also shown to be easily compared with the 2-D distributions. Figures from Fig.10a to Fig.10e correspond to each inlet temperature, and the contour color levels are selected to enhance the temperature differences. And in Fig.10f, five distributions are drawn in one figure, using one common color level for Te1.

Along with the horizontal axis of Fig.9, 16 fuel nozzles are allocated, starting from 11.25 degrees at intervals of 22.5 degrees. And as mentioned before (Fig.3), N1 and N2 nozzles are allocated to the shown positions, which are separated into traverse zones TZ1, TZ2 and TZ3. Each profile has clear shapes corresponding to the positions of the fuel nozzles, and has peak value between each fuel nozzles. But in some sections corresponding to N1-3 of 450K, 500K and 550K, and N1-9 of 500K and 550K, temperature profiles have irregular shapes. These profiles were stable, that is, kept during the traverse measurements for Te1 and Te2. But as the inlet temperature got higher (and combustion load got higher), shape of temperature profiles gradually became distorted, and the differences between Te1 and Te2 also got larger, especially for 600K and 650K conditions. Comparing among three traverse zones, TZ1 looks more stable and the profiles are less sensitive to the inlet temperature. And in TZ2, in which N1 and N2 nozzles were allocated alternately, profiles in the section including N1-1 and N2-5 became distorted as the inlet temperature got higher.

In addition, as other indexes to estimate the exit temperature distribution, profiles of R.T.D.F. (Radial Temperature Distribution Factor) and P.T.F. (Peak Temperature Factor) are calculated at each radial span by following equations.

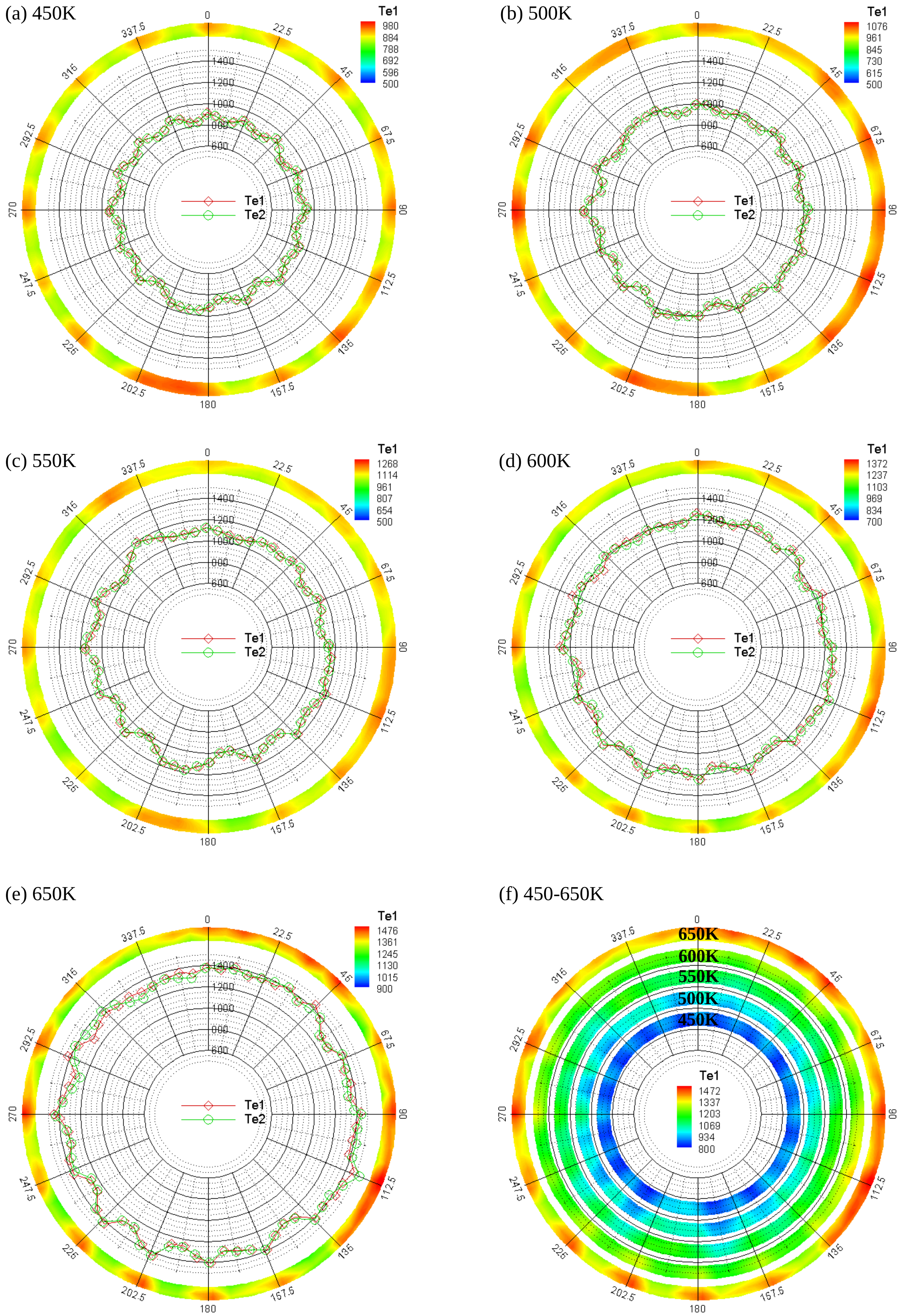

Fig.10. 2D-distributions of exit temperature Te1 and circumferential profiles of Te1 and Te2 of FA2 under parametric test conditions.

$$R.T.D.F. = \frac{T_{4rav} - T_{4av}}{T_{4av} - T_{3av}}, \quad P.T.F. = \frac{T_{4\max} - T_{4av}}{T_{4av} - T_{3av}} \qquad (1)$$

Here, T3 and T4 mean combustor inlet and exit temperature, and subscript "av" means radial and circumferential average and "rav" means circumferential average at a radial span. These factors are calculated for each traverse zone individually, by averaging circumferentially from 11.25 to 78.75 degrees for TZ1, from 90 to 180 degrees for TZ2, and from 202.5 to 337.5 degrees for TZ3, to eliminate the effect of neighboring fuel nozzles. And the transition of R.T.D.F. and P.T.F. profiles for each zone are shown in Fig.11, increasing the inlet temperature as shown in Table.2. These profiles of R.T.D.F. are within the required range from the turbine blade design and limitation (which cannot be shown on this paper). For all zones, slopes of R.T.D.F. got slightly steeper as the inlet temperature increased. And for the TZ1, high exit temperature region shifted to the tip side of the turbine, which indicates that the flame length got longer. On the other hands, the profiles of P.T.F. at each radial span were distorted for TZ3. And the level of P.T.F. profiles were exceeded 0.20 for TZ2 and TZ3. For reference, the averaged P.T.F. values at the 650K condition were 0.184, 0.216 and 0.221 for TZ1, TZ2 and TZ3 respectively. Hence from view point of exit temperature distribution improvement, TZ1 with N2 nozzles was preferable.

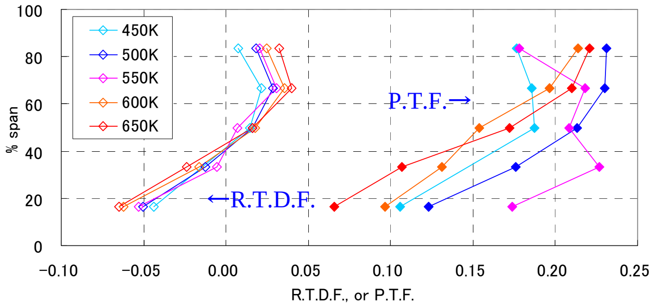

(a) TZ1: N2 nozzles.

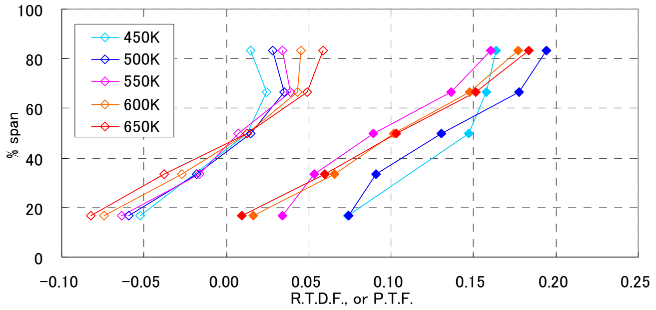

(b) TZ2: N1 and N2 nozzles mixed.

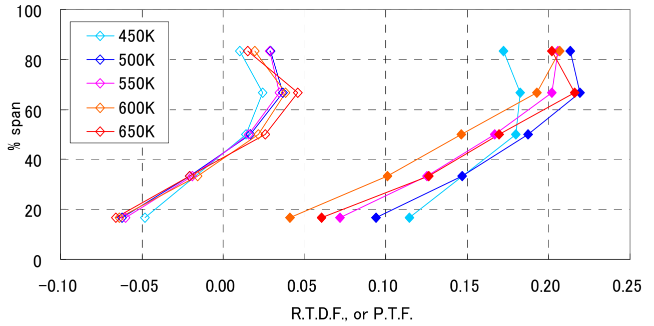

(c) TZ3: N1 nozzles.

Fig.11. Radial profiles of temperature at combustor exit of FA2 under parametric test conditions.

4 Summary

In the TechCLEAN project of JAXA, a series of experimental research has been conducted to develop a small aircraft engine combustor. The designed full annular combustor was tested under the practical conditions of ICAO LTO cycle, and achieved NOx reduction to 38.1% of the ICAO CAEP4 standard.

To investigate the performance of the full annular combustor in detail, parametric experiments were conducted under additional test conditions, increasing inlet air temperature from 450K to 650K with intervals of 50K. By the modified full annular combustor FA2, tuning the air flow ratio of dilution air holes, UHC emission was largely reduced in exchange for increase of NOx emissions.

And some of fuel nozzles were replaced with modified version aiming to improve fuel atomization. From obtained detailed results such as emission characteristics and exit temperature distributions, the modified fuel nozzle N2 showed better performance in NOx reduction and the profile of combustor exit temperature.

Following these results, we would like to investigate the influence of fuel atomization to NOx emissions and to the profile of exit temperature. And then utilize them to the improvement of next full annular combustor models.

Nomenclature

AFR	Air to Fuel Ratio
CAEP	Committee on Aviation Environmental Protection
EINOx	Emission Index of NOx
ICAO	International Civil Aviation Organization
LBO	Lean Blowout
LTO	Landing and Take-Off
MTO	Max Take-Off
P.T.F.	Peak Temperature Factor
R.T.D.F.	Radial Temperature Distribution Factor
T3	Combustor inlet temperature
T4	Combustor exit temperature
TZ1	Traverse Zone 1
UHC	Unburned Hydrocarbon

References

[1] "Aviation and the global atmosphere". *A Special Report of IPCC Working Group I and III.* 1999.

[2] M. Makida, et al. "Preliminary experimental researches to develop a combustor for small class aircraft engine utilizing primary rich combustion approach". ASME GT2006-91156, 2006.

[3] M. Makida, et al. "Optimization of a small aircraft combustor to reduce NOx emissions under practical conditions". ASME GT2007-27969, 2007.

[4] M. Makida, et al. "Development of Full Annular Combustor for Small Aircraft Jet Engine in JAXA Techclean Project", ICAS2008-559, 2008.

[5] Y. Sugiyama, et al. "Research and development of a 1600℃-level combustor with high heat release rate". ISABE95-7099, 1995.

[6] Lefebvre, A. H. *Gas turbine combustion, Second edition*. TAYLOR&FANCIS, Philadelphia, 1998.

[7] Harold C., Simmons et al. "Air-atomizing fuel nozzle". United States Patent, 3980233, Sep.14, 1976.

[8] W. I. Dodos, et al. "Combustion system design". Chap.4 of *Design of modern turbine combustors*. ACADEMIC PRESS, 1990.

[9] N. Zarzalis, et al. "NOx-reduction by rich-lean combustion". AIAA PAPER 92-3339, 1992.

[10] N. K. RIZK and H. C. Mongia. "Three-dimensional NOx modeling for rich/lean combustor". AIAA PAPER 93-0251, 1993.

[11] Hasegawa, et al. "Effect of pressure on emission characteristics in LBG-fueled 1500C-class gas turbine". ASME 97-GT-277, 1997.

[12] P. Griebel, et al. "Experimental investigation of an atmospheric rectangular rich quench lean combustor sector for aeroengines". ASME 97-GT-146, 1997.

[13] J. W. Koopman, et al. "Investigation of a rectangular rich quench lean combustor sector". ASME-98-GT-230, 1998.

[14] Blomeyer, et al. "Mixing zone optimization of a RQL combustor". *J. of Propulsion and Power.* 15, 2, March/April, pp.288-295, 1999.

[15] "Procedure for the continuous sampling and measurement of gaseous, emissions from aircraft turbine engines". SAE ARP1256C, 2006.

Copyright Statement